**Atmospheric
Chemistry
and Physics
Discussions**

**Isotope fractionation
in atmospheric
chloromethane**

A. A. Gola et al.

Kinetic isotope effects in the gas phase reactions of OH and Cl with CH$_3$Cl, CD$_3$Cl, and ^{13}CH$_3$Cl

A. A. Gola[1,*], B. D'Anna[1], K. L. Feilberg[2], S. R. Sellevåg[1], L. Bache-Andreassen[1], and C. J. Nielsen[1]

[1]Department of Chemistry, University of Oslo, P.O.Box 1033 Blindern, N-0315 Oslo, Norway
[2]Department of Chemistry, University of Copenhagen, Universitetsparken 5, DK-2100 Copenhagen, Denmark
[*]permanent address: Department of Physical Chemistry, Medical University of Wroclaw, Pl. Nankiera, 50-140 Wroclaw, Poland

Correspondence to: C. J. Nielsen (c.j.nielsen@kjemi.uio.no)

Title Page

Abstract	Introduction
Conclusions	References
Tables	Figures

|◄ | ►|
◄ | ►
Back | Close

Full Screen / Esc

Print Version

Interactive Discussion

EGU

EGU

Abstract

The kinetic isotope effects in the reactions of CH_3Cl, $^{13}CH_3Cl$ and CD_3Cl with OH radicals and Cl atoms were studied in relative rate experiments at 298 ± 2 K and 1013 ± 10 mbar. The reactions were carried out in a smog chamber using long path FTIR detection and the spectroscopic data analyzed employing a non-linear least squares spectral fitting method using measured high-resolution infrared spectra as well as absorption cross sections from the HITRAN database. The reaction rates of $^{13}CH_3Cl$ and CD_3Cl with OH and Cl were determined relative to CH_3Cl as: $k_{OH+CH3Cl}/k_{OH+13CH3Cl}=1.059\pm0.008$, $k_{OH+CH3Cl}/k_{OH+CD3Cl}=3.9\pm0.4$, $k_{Cl+CH3Cl}/k_{Cl+13CH3Cl}=1.070\pm0.010$ and $k_{Cl+CH3Cl}/k_{Cl+CD3Cl}=4.91\pm0.07$. The uncertainties given are 2σ from the statistical analyses and do not include possible systematic errors. The unusually large ^{13}C kinetic isotope effect in the OH reaction of CH_3Cl has important implications for the global emission inventory of CH_3Cl.

1. Introduction

Chloromethane is the most abundant atmospheric halocarbon with a burden of around 5 Tg nearly all of which is thought to be of natural origin (Khalil and Rasmussen, 1999). Chloromethane is also the only significant natural source of chlorine to the stratosphere (Keene et al., 1999). The global average tropospheric concentration is around 600 pptv (Khalil and Rasmussen, 1999), and with a lifetime with respect to loss by reaction with OH around 1.4 years ($k_{OH}=2.4\times10^{-12}$ $e^{1250/T}$, $k_{OH}(298)=3.6\times10^{-14}$ cm^3 molecules^{-1} s^{-1}) (Sander et al., 2003), the quantified sources can only account for about half of the emissions required to balance the known sinks (Khalil and Rasmussen, 1999). The current understanding of the global budget of CH_3Cl is thus unsatisfactory. Until a few years ago it was thought that most of the global emissions of chloromethane came from the oceans. However, this source can only account for at most 0.5 Tg yr^{-1} (Khalil et al., 1999). Other known and significant sources include 0.9 Tg yr^{-1}

from biomass burning (Lobert et al., 1999), 0.17 Tg yr^{-1} emission from coastal salt marshes (Rhew et al., 2000), 0.15 Tg yr^{-1} from wood-rotting fungi (Watling and Harper, 1998), and 0.16 Tg yr^{-1} from coal combustion, incineration and industrial processes (McCulloch et al., 1999). Evidence was recently presented that abiotic conversion of chloride to chloromethane occurs readily in dead plant material and that this source, not yet quantified, may amount to as much as 2.5 Tg yr^{-1} on a global scale (Hamilton et al., 2003). A more detailed description of the sources of chloromethane in the environment is given by Keppler et al. (2005).

The main quantified removal processes from the troposphere are reaction by OH radicals (3.7±0.9 Tg yr^{-1}) and transport to the stratosphere (0.2 Tg yr^{-1}). Estimates of uptake by soil and subsequent degradation by microorganisms are highly uncertain ranging from 0.2 Tg yr^{-1} (Khalil and Rasmussen, 1999) to 1.6 Tg yr^{-1} (Harper and Hamilton, 2003). Finally, reaction with Cl atoms in the marine boundary layer may remove as much as 0.4 Tg yr^{-1} (Khalil and Rasmussen, 1999).

Stable isotope analysis gives an additional handle to resolve the apparent discrepancy in the source-sink relationship. For chloromethane the global average of the ^{13}C isotope ratio is $\delta^{13}C = -36.2 \pm 0.3‰$ (Thompson et al., 2002) – that is, tropospheric chloromethane is highly depleted in ^{13}C. In this communication we present the first results from kinetic studies of the isotopic fractionation in the atmospheric OH radical and Cl atom loss processes of chloromethane.

2. Experimental

2.1. Reference spectra

FTIR spectra with 0.01 cm^{-1} resolution were recorded with a Bruker IFS 120 FTIR instrument equipped with a liquid N$_2$ cooled InSb semiconductor detector, a KBr beam splitter and a 4000–1800 cm^{-1} band pass filter. To achieve an acceptable signal/noise ratio in the resultant spectra 128 scans were co-added. The partial pressures

Isotope fractionation in atmospheric chloromethane

A. A. Gola et al.

EGU

of chloromethane isotopologues were in the range 10–30 mbar and the cell (10 cm, CaF_2 windows) was filled to 1013 mbar with synthetic air (Air Liquide, 99.998%).

2.2. Relative rate experiments

The kinetic study was carried out by the relative rate method in a static gas mixture, in which the removal of the reacting species is measured simultaneously as a function of reaction time. Consider two simultaneous bimolecular reactions with the rate coefficients k_A and k_B:

$$A + X \xrightarrow{k_A} \text{products} \tag{1}$$

$$B + X \xrightarrow{k_B} \text{products} \tag{2}$$

Assuming that there are no other loss processes than these reactions and that there are no other processes producing the reactants, the following relation is valid:

$$\ln\left\{\frac{[A]_0}{[A]_t}\right\} = \frac{k_A}{k_B} \ln\left\{\frac{[B]_0}{[B]_t}\right\} \tag{3}$$

where $[A]_0$, $[A]_t$, $[B]_0$ and $[B]_t$ denote the concentrations of the compounds A and B at times zero and t, respectively. A plot of $\ln([A]_0/[A]_t)$ vs. $\ln([B]_0/[B]_t)$ will thus give the relative reaction rate coefficient $\alpha = k_A/k_B$ as the slope, or in terms of the fractionation constant, ε, of the loss process: $\varepsilon = (\alpha - 1) \times 1000‰$.

The experiments were carried out in a 250 L electropolished stainless steel smog chamber equipped with a White type multiple reflection mirror system with a 120 m optical path length for rovibrationally resolved infrared spectroscopy. The infrared spectra were recorded with Bruker IFS 88 and IFS 66v FTIR instruments equipped with a liquid nitrogen cooled InSb detector. As a standard 128 scans were co-added at a nominal resolution of $0.125\,\text{cm}^{-1}$ and Fourier transformed using boxcar apodization. Periods of data collection (ca. 10 min.) were alternated with UV photolysis (see below) and a waiting period of 2 min. until 40–60% of the initial CH_3Cl was consumed. For a given gas

Isotope fractionation in atmospheric chloromethane

A. A. Gola et al.

mixture the entire experiment typically lasted 1–2 h for the Cl atom reactions and 4–6 h for the OH radical reactions. The reaction chamber was equipped with UV photolysis lamps mounted in a quartz tube inside the chamber, and all experiments were carried out in synthetic air (AGA 99.999% purity; CH_4, CO and $NO_x < 100$ ppbv) at 298 ± 2 K and 1013 ± 10 mbar. The temperature was monitored on the chamber wall and it remained constant for the duration of the experiments. Each of the OH and Cl experiments was carried out several times for different mixtures of chloromethane isotopologues: $CH_3Cl + CD_3Cl$ and $CH_3Cl + {}^{13}CH_3Cl$.

2.3. Data analysis

The experimental spectra were analysed using a global non-linear least squares spectral fitting procedure, NLM (Griffith, 1996). The spectral features used in the analyses were the C-H stretching bands in the 2825–3100 cm^{-1} region and the C-D stretching bands in the 2025–2260 cm^{-1} region. The spectral data needed for the fitting procedure were taken from the HITRAN database (HCl, H_2O, N_2O, CO, CO_2, CH_4 and the ν_2 band of O_3); for CH_3Cl, ${}^{13}CH_3Cl$, CD_3Cl and the overtone/combinations bands of O_3 (for which HITRAN does not yet include data for the isotopologues) experimental high-resolution IR spectra were used.

The analysis of the FTIR spectra produced accurate values for the relative change in concentrations. The data from independent experiments were analysed according to Eq. (3) using a weighted least squares procedure which includes uncertainties in both reactant concentrations (York, 1966); the uncertainties in the reactant concentrations were taken as the standard deviations from the least squares fitting of the experimental infrared spectra. The analyses were carried out in two steps: (i) data from the individual experiments were fitted to a straight line with no constraints imposed. If there was no statistical significance to the intercept $\neq 0$, the first data point (t = zero) was taken out and the remaining (n–1) data points were then fitted jointly with data from the other experiments to a straight line forced through the origin. If a dataset showed a statistical

significant intercept ≠ 0, the dataset was disregarded (the experiment was repeated).

2.4. Chemicals and radical production

CH_3Cl (>99.5%, Aldrich), $^{13}CH_3Cl$ (99 atom % 13C, ISOTEC Inc.) and CD_3Cl (99.5 atom % D, ISOTEC Inc.) were used as received without further purification. Typical
5 volume fractions of the chloromethane isotopologues were 3–4 ppm.

Hydroxyl radicals were generated by photolysis of ozone/H_2 mixtures; typical volume fractions of H_2 (AGA 4.5) and ozone were 2×10^3 ppm and 300 ppm, respectively. Ozone was produced from O_2 (AGA 4.5) by using a MK II Ozone generator from BOC that converts approximately 5% of the oxygen gas flow to ozone. The photodissociation
10 of ozone was accomplished by a Philips TUV 30W lamp ($\lambda_{max} \sim 254$ nm) mounted in a quartz tube in the smog chamber; photolysis was done in time intervals of 1–30 min.

$$O_3 + h\nu(\lambda \sim 254 \text{ nm}) \rightarrow O(^1D) + O_2 \tag{4}$$

$$O(^1D) + H_2 \rightarrow OH + H \tag{5}$$

$$H + O_3 \rightarrow OH + O_2 \tag{6}$$

15 This OH production scheme produces not only OH radicals in the ground-state but also in excited vibrational states (Aker and Sloan, 1986; Huang et al., 1986; Streit et al., 1976). The collision quenching rate coefficients of OH by N_2 and O_2 are of the order of 10^{-15} and 10^{-13} cm^3 molecule^{-1} s^{-1}, respectively (D'Ottone et al., 2004). However, the mixing ratios of O_2 and N_2 are five orders of magnitude larger than those
20 of the chloromethane isotopologues, and one may therefore safely assume that the latter react exclusively with OH in the vibrational ground state.

The chlorine atoms were generated by photolysis of Cl_2 using Philips TLD-08 fluorescence lamps ($\lambda_{max} \sim 350$ nm). In this wavelength region the Cl atoms produced were in the ground state (see later). The Cl_2 was a standard laboratory grade compound
25 (AGA 2.8) and was purified by two freeze-pump-thaw cycles prior to use. Typical volume fractions were 10–20 ppm Cl_2.

EGU

The experiments were carried out under low NO_x conditions ($NO_x < 100$ pptv) and according to previous product studies (Bilde et al., 1999; Catoire et al., 1994; Kaiser and Wallington, 1994; Niki et al., 1980; Sanhueza and Heicklen, 1975; Wallington et al., 1995) the Cl initiated oxidation of CH_3Cl will, under the present reaction conditions,

5 essentially proceed via Reactions (7–12)

$$Cl + CH_3Cl \rightarrow CH_2Cl + HCl \tag{7}$$
$$CH_2Cl + O_2 \rightarrow CH_2ClO_2 \tag{8}$$

$$CH_2ClO_2 + CH_2ClO_2 \rightarrow CH_2ClO + CH_2ClO + O_2 \tag{9a}$$
10 $$\rightarrow HC(O)Cl + CH_2ClOH + O_2 \tag{9b}$$

$$CH_2ClO_2 + HO_2 \rightarrow HC(O)Cl + H_2O + O_2 \tag{10a}$$
$$\rightarrow CH_2ClOOH + O_2 \tag{10b}$$

15 $$CH_2ClO + M \rightarrow HCO + HCl + M \tag{11}$$
$$CH_2ClO + O_2 \rightarrow HC(O)Cl + HO_2 \tag{12}$$

During the Cl atom reaction with CH_3Cl OH radicals will eventually be generated from the HO_2 radicals and thereby influence the kinetics. We therefore modelled the reactions in the static reactor using FACSIMILE (MCPA Software Ltd) to find the optimum

20 starting conditions. The basic model of our reactor, given as supporting information, consists of around 200 equations describing O_x, HO_x, NO_x, FO_x, ClO_x, BrO_x and CH_4-related "background" reactions in the chamber; the rate coefficient data have been taken from the latest JPL (Sander et al., 2003) and IUPAC (Atkinson, 2004) kinetic data evaluations (the photolysis rates of photo-labile constituents were determined ex-

25 perimentally in our laboratory). In addition we included the reactions describing the Cl and OH initiated oxidation of CH_3Cl as indicated by Reactions (7–12) and the subsequent degradation reaction reactions of HC(O)Cl (Libuda et al., 1990). Using 5 ppm

CH$_3$Cl and 10 ppm Cl$_2$ as starting conditions, the model indicated that the loss of CH$_3$Cl due to reactions with OH radicals was less than 1‰ of the total loss. The model also predicted that the concentration of HC(O)Cl formed could be as high as 0.5 ppm; the absorption lines of this molecule could therefore interfere with the analyses of the C-H/C-D stretching regions of the spectrum. We therefore also carried out experiments using the Philips TUV 30W lamp ($\lambda_{max} \sim 253.7$ nm) which will photolyse HC(O)Cl. At this wavelength Cl atoms can be formed in the excited spin-orbit state ^{2}P$_{1/2}$, which is ca. 882 cm^{-1} above the ground state ^{2}P$_{3/2}$. The quenching rate coefficients of Cl(^{2}P$_{1/2}$) by O$_2$ and N$_2$ are of the order of 10^{-13} and 10^{-15} cm^3 molecule^{-1} s^{-1} (Tyndall et al., 1995). However, one may safely assume that only Cl(^{2}P$_{3/2}$) will react with CH$_3$Cl since the mixing ratios of O$_2$ and N$_2$ are five orders of magnitude larger than that of CH$_3$Cl.

The formation of HC(O)Cl can in principle also affect the kinetic study of the CH$_3$Cl reaction with OH since Cl atoms are released in the degradation of HC(O)Cl (either through photolysis of HC(O)Cl or reaction with OH and decomposition of the ClCO radical). The FACSIMILE model indicated that the loss of CH$_3$Cl due to reactions with Cl atoms is at most 1‰ because the Cl atoms are effectively scavenged by the presence of 2×10^3 ppm H$_2$ in the reaction chamber.

3. Results

Figure 1 shows the obtained FT-IR spectra of a CH$_3$Cl and ^{13}CH$_3$Cl in the CH stretching region. The fundamental ν_1(A$_1$) parallel band is situated around 2968 cm^{-1}, the ν_4(E) perpendicular band around 3039 cm^{-1}, and the $2\nu_5$(A$_1$+E) overtone around 2879 cm^{-1}. Although the ^{12}C-^{13}C isotopic shifts are small for the three bands (around −4, −9 and −5 cm^{-1}, respectively) the rotational fine structures of the fundamentals are sufficiently different that isotopic mixtures can be quantified from infrared spectra of mixtures containing O$_3$ obtained at a spectral resolution of 0.125 cm^{-1}. The CD stretching modes of CD$_3$Cl are not shown but are found around 2160 cm^{-1} (ν_1(A$_1$))

Isotope fractionation in atmospheric chloromethane

A. A. Gola et al.

Title Page

Abstract | Introduction

Conclusions | References

Tables | Figures

◄◄ | ►►

◄ | ►

Back | Close

Full Screen / Esc

Print Version

Interactive Discussion

EGU

and 2285 cm^{-1} (ν_4(E)), and CD_3Cl is easily quantified in mixtures with N_2O, CO_2, CO and O_3.

3.1. Cl atom reactions

Two sets of photolysis experiments were performed: (i) photolysis at λ_{max}~350 nm and (ii) photolysis at λ_{max}~254 nm. The results from these experiments were not significantly different. This suggests that either the wall loss of HC(O)Cl in our chamber is larger than that reported by Libuda et al. (1990), or that the absorption lines of HC(O)Cl are too weak to affect our spectral analyses (a rough estimate from the IR spectrum of Libuda et al. predicts that 0.5 ppm of HC(O)Cl in our system should have an absorption of 2×10^{-3} in the C-H stretching region, which is in the noise level). An example of the FT-IR spectra obtained from the study of the $^{12}CH_3Cl$/$^{13}CH_3Cl$ reaction with Cl atoms and the result from a non-linear least squares spectral fit using data from the HITRAN database and high-resolution spectra of the reactants is shown in Fig. 2, while Fig. 3 shows a plot of $\ln\{[^{12}CH_3Cl]_0/[^{12}CH_3Cl]_t\}$ vs. $\ln\{[^{13}CH_3Cl]_0/[^{13}CH_3Cl]_t\}$ during the reaction with Cl atoms; analysis of data from five independent experiments according to Eq. (3) gives $k(Cl+^{12}CH_3Cl)/k(Cl+^{13}CH_3Cl)=1.070\pm0.010$ (Table 1), where the error quoted in the relative rate corresponds to the 2σ error of the statistical analysis only.

The infrared spectrum of the CD stretching region during an experiment with Cl atom reaction with CH_3Cl and CD_3Cl is shown in Fig. 4. The ν_4(E) mode at 2285 cm^{-1} is partly overlapped by the strongly absorbing $\nu_3(\Sigma_g^+)$ mode of CO_2 around 2349 cm^{-1} and this part of the spectrum was therefore not included in the spectral fitting. The decays of CH_3Cl and CD_3Cl during the reaction with Cl atoms are shown in Fig. 5 in the form of $\ln\{[CH_3Cl]_0/[CH_3Cl]_t\}$ vs. $\ln\{[CD_3Cl]_0/[CD_3Cl]_t\}$ from which $k(Cl+CH_3Cl)/k(Cl+CD_3Cl)=4.91\pm0.07$ (Table 1) was derived from data of 2 independent experiments.

EGU

3.2. OH radical reactions

Numerous experiments were carried out with OH reactions with $^{12}CH_3Cl$ and $^{13}CH_3Cl$. Because the reaction is slow, $k_{OH}(298\,K)=3.6\times10^{-14}\,cm^3\,molecule^{-1}\,s^{-1}$ (Sander et al., 2003), rather high initial ozone concentrations are needed to achieve a reasonable degree of reaction. This, on the other hand, makes the spectral analyses more demanding. Figure 6 shows the spectrum of a reaction mixture containing ca. 2.5 ppm of each of $^{12}CH_3Cl$ and $^{13}CH_3Cl$, and ca. 600 ppm O_3 (and 1000 ppm H_2) in purified air. The spectrum is dominated by 4 ozone bands ($\nu_1+2\nu_3$, $3\nu_3$, $\nu_1 + \nu_2 + \nu_3$, $\nu_2+2\nu_3$) of which the $3\nu_3$ band at 3046 cm^{-1} obscures the $\nu_4(E)$ perpendicular bands and overlaps the $\nu_1(A_1)$ parallel bands of the $^{12}CH_3Cl$ and $^{13}CH_3Cl$. However, all spectral details can be accounted for as the residual of the spectral fitting shows. Figure 7 summarizes the results of the kinetic data from 4 independent experiments from which we extract $k(OH+^{12}CH_3Cl)/k(OH+^{13}CH_3Cl)=1.059\pm0.008$.

Figure 8 shows the spectral region used for analyzing the removal of CD_3Cl from the reactor by OH radicals. Although the $\nu_4(E)$ band is overlapped by the ν_3 band of $^{13}CO_2$, the $2\nu_5(A_1+E)$ band is completely covered by the $\nu_1 + \nu_3$ band of O_3, and the $\nu_1(A_1)$ band of CD_3Cl is overlapped by the $\nu_1 + \nu_3$ band of O_3 as well as by vibration-rotation lines of the N_2O ν_3 band and of the CO fundamental, all spectral details are accounted for. However, the CD_3Cl+OH reaction is rather slow ($9.2\times10^{-15}\,cm^3\,molecule^{-1}\,s^{-1}$, this work) and only around 10% of the initial amount of CD_3Cl reacted during the experiments. We have therefore only been able to determine the relative rate of reaction with an uncertainty of 10% from 4 independent experiments; $k(OH+CH_3Cl)/k(OH+CD_3Cl)=3.9\pm0.4$ (Table 1).

EGU

4. Conclusions

The kinetic isotope effects in the Cl atom and OH radical reactions with chloromethane should be compared to those of the analogue reactions of methane which has been the subject of numerous studies (Boone et al., 2001; Chiltz et al., 1963; Clyne and Walker, 1973; Crowley et al., 1999; Feilberg et al., 2005a; Gierczak et al., 1997; Matsumi et al., 1997; Saueressig et al., 1995, 1996, 2001; Tyler et al., 2000; Wallington and Hurley, 1992) – Table 1 includes the latest results. The ^{13}C KIE in the Cl reaction of chloromethane is nearly the same as in methane, 1.058 (Feilberg et al., 2005a). In contrast, the ^{13}C KIE in the OH reaction is more than 1 order of magnitude larger than observed for methane, 1.0039 (Saueressig et al., 2001). Also the KIE's of the CD_3Cl differs significantly from those of fully deuterated methane. Especially the high value for the ^{13}C KIE in the OH reaction is on its own somewhat surprising. We have, however, recently obtained similar values of the KIEs in the Cl atom and OH radical reactions with CH_3Br (Nikitine et al., 2005[1]), CH_2Cl_2 (Iannetta et al., 2005[2]) and CH_3OH (Feilberg et al., 2005b[3]), and suggest that it is the ^{13}C KIE of the OH reaction with methane that is unusually small rather than the ^{13}C KIE of the OH radical reaction with chloromethane being 'surprisingly' large. Preliminary variational transition state calculations also support this view (Sellevåg et al., 2005[4]).

---

[1]Nikitine, T., Bache-Andreassen, L., D'Anna, B., and Nielsen, C. J.: Kinetic isotope effects in the gas phase reactions of OH and Cl with CH_3Br, CD_3Br and $13CH_3Br$, J. Chem. Phys., to be published, 2005.

[2]Iannetta, C., Gola, A. A., Bache-Andreassen, L., and Nielsen, C. J.: Kinetic isotope effects in the gas phase reactions of OH and Cl with CH_2Cl_2, $CHDCl_2$, CD_2Cl_2 and $13CH_2Cl_2$, J. Chem. Phys., to be published, 2005.

[3]Feilberg, K. L., Johnson, M. S., and Nielsen, C. J.: 13C, 18O and D fractionation effects in the reactions of methanol with Cl and OH radicals, J. Chem. Phys., A, submitted, 2005b.

[4]Sellevåg, S. R., Nyman, G., and Nielsen, C. J.: Study of the carbon-13 and deuterium kinetic isotope effects in the Cl and OH reactions of CH_4 and CH_3Cl, J. Phys. Chem. A,

EGU

Only half of the chloromethane needed to balance the known sinks have so far been quantified by field measurements (Khalil and Rasmussen, 1999). The ^{13}C fractionation in the OH reaction with chloromethane can be used to constrain the budget and to narrow down the possible source(s). Tropospheric chloromethane is highly depleted in ^{13}C with a global average of the of $\delta^{13}C=-36.2\pm0.3‰$ (Thompson et al., 2002) and an OH fractionation of $\varepsilon^{13}C=59\pm8‰$ requires a large and extremely depleted ^{13}C source. This is discussed in detail by Keppler et al. (2005).

Supplementary material

Supplementary material is available under:
http://www.copernicus.org/EGU/acp/acpd/5/3873/acpd-5-3873-sp.pdf.

References

Aker, P. M. and Sloan, J. J.: The initial product vibrational energy distribution in the reaction between atomic oxygen(1D2) and hydrogen molecule, J. Chem. Phys., 85 (3), 1412–1417, 1986.

Atkinson, R., Baulch, D. L., Cox, R. A., Crowley, J. N., Hampson Jr., R. F., Hynes, R. G., Jenkin, M. E., Kerr, J. A., Rossi, M. J., and Troe, J.: Summary of evaluated kinetic and photochemical data for atmospheric chemistry; IUPAC Subcommittee on Gas Kinetic Data Evaluation for Atmospheric Chemistry, Web Version July 2004.

submitted, 2005.

EGU

Bilde, M., Orlando, J. J., Tyndall, G. S., Wallington, T. J., Hurley, M. D., and Kaiser, E. W.: FT-IR Product Studies of the Cl-Initiated Oxidation of CH3Cl in the Presence of NO, J. Phys. Chem. A, 103 (20), 3963–3968, 1999.

Boone, G. D., Agyin, F., Robichaud, D. J., Tao, F.-M., and Hewitt, S. A.: Rate Constants for the Reactions of Chlorine Atoms with Deuterated Methanes: Experiment and Theory, J. Phys. Chem. A, 105 (9), 1456–1464, 2001.

Catoire, V., Villenave, E., Rayez, M. T., and Lesclaux, R.: Kinetic studies of the CH2ClO2 and CH2BrO2 radical reactions, Reaction of the CH2ClO radical, European Commission, [Report] EUR (15609, Physico-Chemical Behaviour of Atmospheric Pollutants, Vol. 1), 411–416, 1994.

Chiltz, G., Eckling, R., Goldfinger, P., Huybrechts, G., Johnston, H. S., Meyers, L., and Verbeke, G.: Kinetic isotope effect in photochlorination of H2, CH4, CHCl3, and C2H6, J. Chem. Phys., 38, 1053–1061, 1963.

Clyne, M. A. A. and Walker, R. F.: Absolute rate constants for elementary reactions in the chlorination of methane, methane-d4, methyl chloride, methylenechloride, chloroform, chloroform-d, and bromotrichloromethane, J. Chem. Soc., Faraday Transactions 1: Physical Chemistry in Condensed Phases, 69 (9), 1547–1567, 1973.

Crowley, J. N., Saueressig, G., Bergamaschi, P., Fischer, H., and Harris, G. W.: Carbon kinetic isotope effect in the reaction CH4 + Cl: a relative rate study using FTIR spectroscopy, Chem. Phys. Lett., 303 (3,4), 268–274, 1999.

D'Ottone, L., Bauer, D., Campuzano-Jost, P., Fardy, M., and Hynes, A. J.: Vibrational deactivation studies of OH X2P (v = 1-5) by N2 and O2, Phys. Chem. Chem. Phys., 6 (17), 4276–4282, 2004.

Feilberg, K. L., Griffith, D. W. T., Johnson, M. S., and Nielsen, C. J.: The 13C and D kinetic isotope effects in the reaction of CH4 with Cl, Int. J. Chem. Kinetics, 37 (2), 110–118, 2005a.

Gierczak, T., Talukdar, R. K., Herndon, S., Vaghjiani, G. L., and Ravishankara, A. R.: Rate Coefficients for the Reactions of Hydroxyl Radicals with Methane and Deuterated Methanes, J. Phys. Chem. A, 101 (17), 3125–3134, 1997.

Griffith, D. W. T.: Synthetic calibration and quantitative analysis of gas-phase FT-IR spectra, Applied Spectroscopy, 50, 59–70, 1996.

Hamilton, J. T. G., McRoberts, W. C., Keppler, F., Kalin, R. M., and Harper, D. B.: Chloride methylation by plant pectin: An efficient environmentally significant process, Science, 301 (5630), 206–209, 2003.

Isotope fractionation in atmospheric chloromethane

A. A. Gola et al.

EGU

Harper, D. B. and Hamilton, J. T. G.: The Global cycles of the naturally-occuring mono-halomethanes, in: The Handbook of Environmental Chemistry Vol. 3/P, Natural production of organohalogen compounds, edited by: Gribble, G. W., 17–14, 2003.

Huang, Y., Gu, Y., Liu, C., Yang, X., and Tao, Y.: The nascent product vibrational energy distribution of the reaction O(1D) + H2 by the grating selection chemical laser technique, Chem. Phys. Lett., 127 (5), 432–437, 1986.

Kaiser, E. W. and Wallington, T. J.: FTIR Product Study of the Cl-Initiated Oxidation of CH3Cl: Evidence for HCl Elimination from the Chloromethoxy Radical, J. Phys. Chem., 98 (22), 5679–5685, 1994.

Keene, W. C., Khalil, M. A. K., Erickson III, D. J., McCulloch, A., Graedel, T. E., Lobert, J. M., Aucott, M. L., Gong, S. L., Harper, D. B., Kleiman, G., Midgley, P., Moore, R. M., Seuzaret, C., Sturges, W. T., Benkovitz, C. M., Koropalov, V., Barrie, L. A., and Li, Y. F.: Composite global emissions of reactive chlorine from anthropogenic and natural sources: Reactive Chlorine Emissions Inventory, J. Geophys. Res., 104(D7), 8429–8440, 1999.

Keppler, F., Harper, D. B., Röckmann, T., and Hamilton, J. T. G.: New insight into the atmospheric chloromethane budget gained using stable carbon isotope ratios, Atmos. Chem. Phys. Discuss., 5, 3899–3919, 2005.

Khalil, M. A. K., Moore, R. M., Harper, D. B., Lobert, J. M., Erickson, D. J., Koropalov, V., Sturges, W. T., and Keene, W. C.: Natural emissions of chlorine-containing gases: Reactive Chlorine Emissions Inventory, J. Geophys. Res., 104(D7), 8333–8346, 1999.

Khalil, M. A. K. and Rasmussen, R. A.: Atmospheric methyl chloride, Atmos. Environ., 33 (8), 1305–1321, 1999.

Libuda, H. G., Zabel, F., Fink, E. H., and Becker, K. H.: Formyl chloride: UV absorption cross sections and rate constants for the reactions with chlorine atom and hydroxyl radical, J. Phys. Chem., 94 (15), 5860–5865, 1990.

Lobert, J. M., Keene, W. C., Logan, J. A., and Yevich, R.: Global chlorine emissions from biomass burning: Reactive Chlorine Emissions Inventory, J. Geophys. Res., 104(D7), 8373–8389, 1999.

Matsumi, Y., Izumi, K., Skorokhodov, V., Kawasaki, M., and Tanaka, N.: Reaction and Quenching of Cl(2Pj) Atoms in Collisions with Methane and Deuterated Methanes, J. Phys. Chem. A, 101 (7), 1216–1221, 1997.

McCulloch, A., Aucott, M. L., Benkovitz, C. M., Graedel, T. E., Kleiman, G., Midgley, P. M., and Li, Y.-F.: Global emissions of hydrogen chloride and chloromethane from coal combustion,

Title Page

Abstract | Introduction

Conclusions | References

Tables | Figures

◄ | ►►

◄ | ►

Back | Close

Full Screen / Esc

Print Version

Interactive Discussion

EGU

incineration and industrial activities: Reactive Chlorine Emissions Inventory, J. Geophys. Res., 104(D7), 8391–8403, 1999.

FACSIMILE for Windows, Version 4.0.31, MCPA Software Ltd.

Niki, H., Maker, P. D., Savage, C. M., and Breitenbach, L. P.: An FTIR (Fourier Transform IR) study of the chlorine atom-initiated oxidation of dichloromethane and chloromethane, Int. J. Chem. Kin., 12 (12), 1001–1012, 1980.

Rhew, R. C., Miller, B. R., and Weiss, R. F.: Natural methyl bromide and methyl chloride emissions from coastal salt marshes, Nature, 403 (6767), 292–295, 2000.

Sander, S. P., Friedl, R. R., Golden, D. M., Kurylo, M. J., Huie, R. E., Orkin, V. L., Moortgat, G. K., Ravishankara, A. R., Kolb, C. E., Molina, M. J., and Finlayson-Pitts, B. J.: Chemical Kinetics and Photochemical Data for Use in Atmospheric Studies, Evaluation Number 14, National Aeronautics and Space Administration, Jet Propulsion Laboratory, California Institute of Technology, Pasadena, California, 2003.

Sanhueza, E. and Heicklen, J.: Chlorine-atom sensitized oxidation of dichloromethane and chloromethane, J. Phys. Chem., 79 (1), 7–11, 1975.

Saueressig, G., Bergamaschi, P., Crowley, J. N., Fischer, H., and Harris, G. W.: Carbon kinetic isotope effect in the reaction of CH4 with Cl atoms, Geophys. Res. Lett., 22(10), 1225–1228, 1995.

Saueressig, G., Bergamaschi, P., Crowley, J. N., Fischer, H., and Harris, G. W.: D/H kinetic isotope effect in the reaction CH4 + Cl, Geophys. Res. Lett., 23(24), 3619–3622, 1996.

Saueressig, G., Crowley, J. N., Bergamaschi, P., Bruhl, C., Brenninkmeijer, C. A. M., and Fischer, H.: Carbon 13 and D kinetic isotope effects in the reactions of CH4 with O(1D) and OH: New laboratory measurements and their implications for the isotopic composition of stratospheric methane, J. Geophys. Res., 106(D19), 23 127–23 138, 2001.

Streit, G. E., Whitten, G. Z., and Johnston, H. S.: The fate of vibrationally excited hydroxyl radicals, HO (v<9), in the stratosphere, Geophys. Res. Lett., 3 (9), 521–523, 1976.

Thompson, A. E., Anderson, R. S., Rudolph, J., and Huang, L.: Stable carbon isotope signatures of background tropospheric chloromethane and CFC113, Biogeochemistry, 60 (2), 191–211, 2002.

Tyler, S. C., Ajie, H. O., Rice, A. L., Cicerone, R. J., and Tuazon, E. C.: Experimentally determined kinetic isotope effects in the reaction of CH4 with Cl: implications for atmospheric CH4, Geophys. Res. Lett., 27(12), 1715–1718, 2000.

Tyndall, G. S., Orlando, J. J., and Kegley-Owen, C. S.: Rate coefficients for quenching of

Isotope fractionation in atmospheric chloromethane

A. A. Gola et al.

EGU

Cl(2P1/2) by various atmospheric gases, J. Chem. Soc., Faraday Transactions, 91 (18), 3055–3061, 1995.

Wallington, T. J. and Hurley, M. D.: A kinetic study of the reaction of chlorine atoms with chlorofluoroethanes, deuterated methanes, and chloromethane-d3 (CF3CHCl2, CF3CH2F, CFCl2CH3, CF2ClCH3, CHF2CH3, CH3D, CH2D2, CHD3, CD4, and CD3Cl) at 295+-2 K, Chem. Phys. Lett., 189 (4-5), 437–442, 1992.

Wallington, T. J., Orlando, J. J., and Tyndall, G. S.: Atmospheric Chemistry of Chloroalkanes: Intramolecular Elimination of HCl from Chloromethoxy radicals over the Temperature Range 264–336 K, J. Phys. Chem., 99 (23), 9437–9442, 1995.

Watling, R. and Harper, D. B.: Chloromethane production by wood-rotting fungi and an estimate of the global flux to the atmosphere, Mycological Research, 102 (7), 769–787, 1998.

York, D.: Least-squares fitting of a straight line, Can. J. Phys., 44, 1079–1086, 1966.

Isotope fractionation in atmospheric chloromethane

A. A. Gola et al.

Title Page

Abstract | Introduction

Conclusions | References

Tables | Figures

◄ | ►

◄ | ►

Back | Close

Full Screen / Esc

Print Version

Interactive Discussion

EGU

Table 1. Kinetic isotope effects in the reactions of chloromethane and methane with Cl atoms and OH radicals.

k_A/k_B	Cl	OH
$CH_3Cl/^{13}CH_3Cl$	1.070 ± 0.010	1.059 ± 0.008
CH_3Cl/CD_3Cl	4.91 ± 0.07	3.9 ± 0.4
$CH_4/^{13}CH_4$	1.058 ± 0.002 [a]	1.0039 ± 0.0004 [b]
CH_4/CH_3D	1.459 ± 0.006 [a]	1.294 ± 0.018 [c]
CH_4/CH_2D_2	2.43 ± 0.01 [a]	1.81 ± 0.28 [c]
CH_4/CHD_3	4.73 ± 0.04 [a]	3.30 ± 0.50 [c]
CH_4/CD_4	14.7 ± 0.2 [a]	7.36 ± 0.88 [c]

[a] Feilberg et al. (2005a)
[b] Saueressig et al. (2001)
[c] Gierczak et al. (1997)
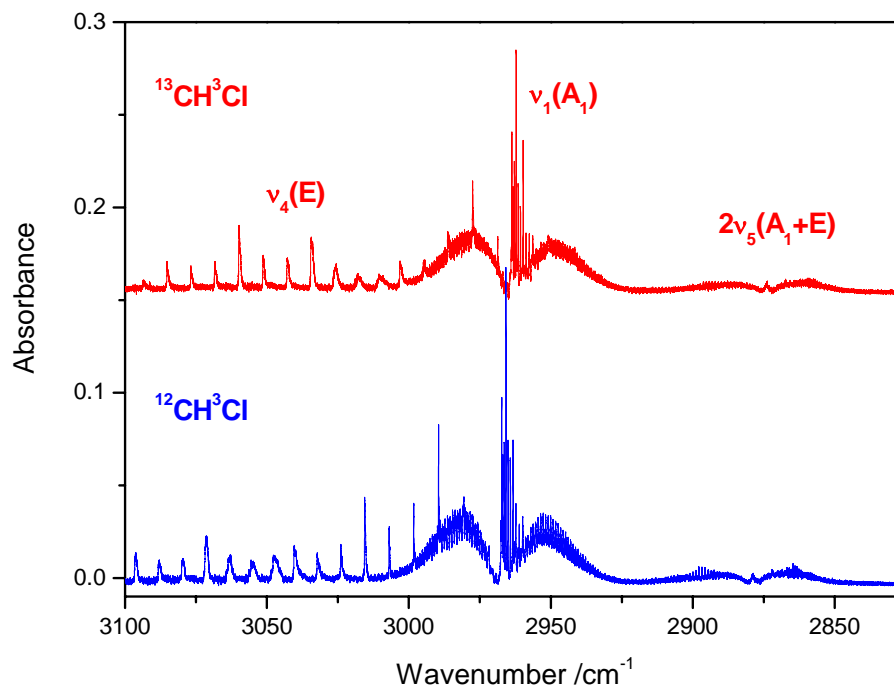
Fig. 1. FT-IR spectra in the CH stretching region of a CH_3Cl and $^{13}CH_3Cl$ showing the fundamental ν_1 parallel band around $2960\,cm^{-1}$, the ν_4 perpendicular band around $3040\,cm^{-1}$, as well as the $2\nu_5$ overtone around $2875\,cm^{-1}$. Spectral resolution: $0.01\,cm^{-1}$.
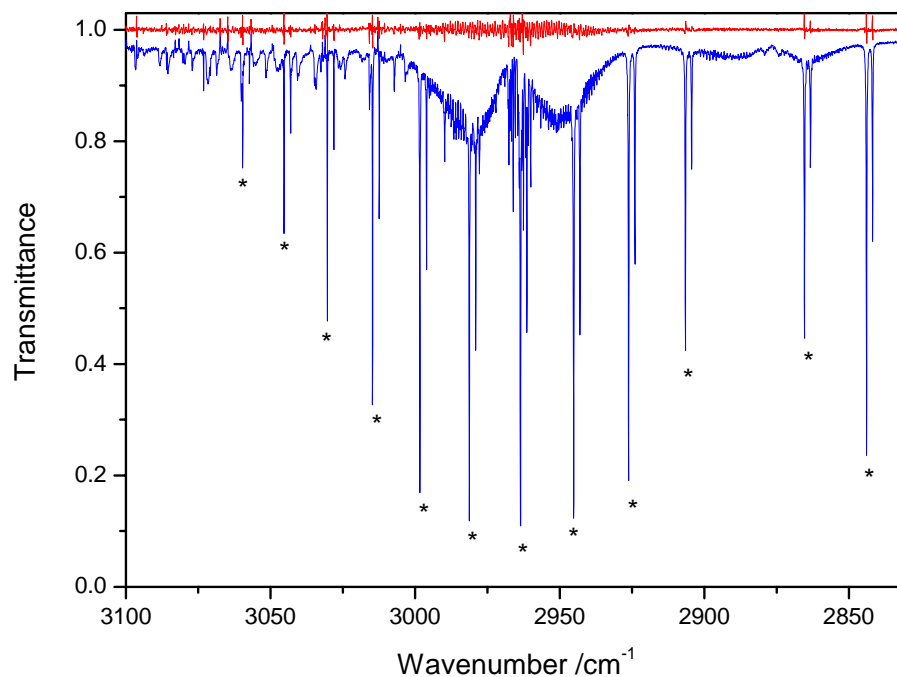
Fig. 2. FT-IR spectrum of the CH stretching region of a CH_3Cl and $^{13}CH_3Cl$ mixture during reaction with Cl atoms. Total photolysis time: 2 min. Compounds included in the spectral analysis: $^{12}CH_3Cl$, $^{13}CH_3Cl$, H_2O and HCl. (*) Bands due to HCl.
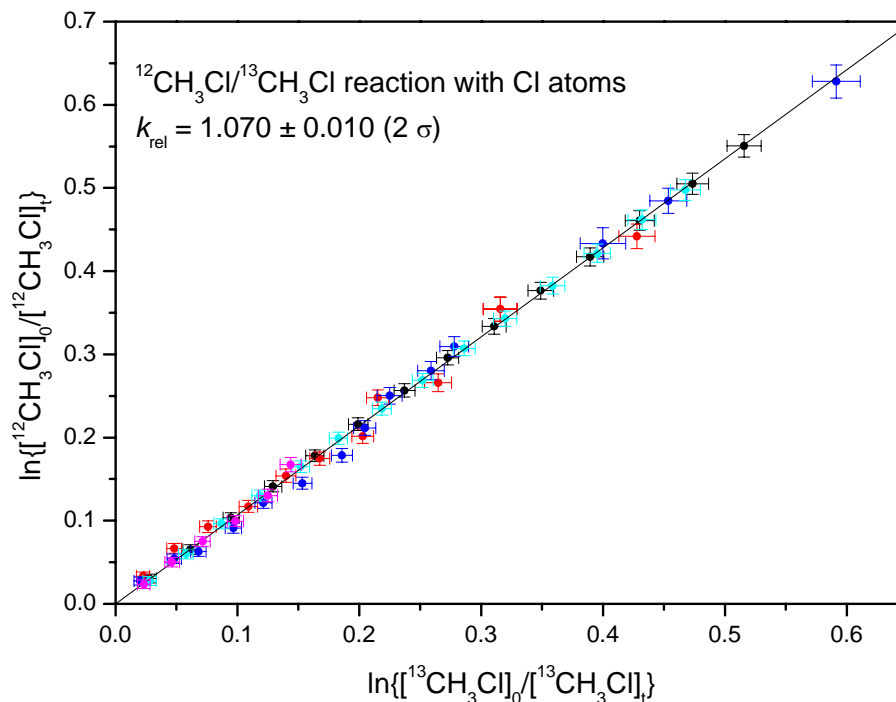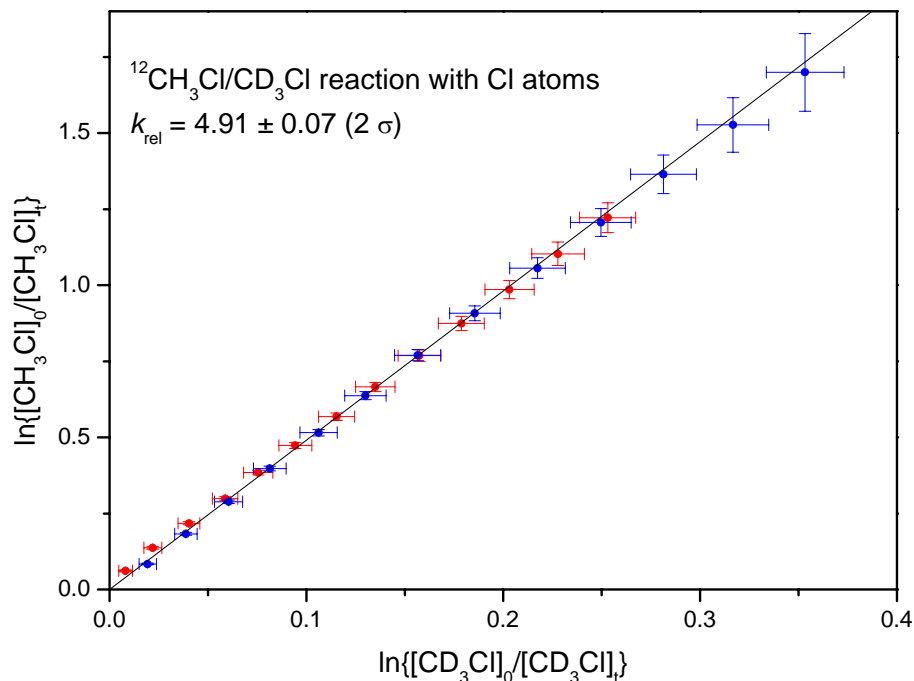
Fig. 3. Decays of $^{12}CH_3Cl$ and $^{13}CH_3Cl$ during reaction with Cl atoms at 1013 mbar and 298 K plotted in the form of $\ln\{[^{12}CH_3Cl]_0/[^{12}CH_3Cl]_t\}$ vs. $\ln\{[^{13}CH_3Cl]_0/[^{13}CH_3Cl]_t\}$. 60 data points from 5 independent experiments (colour coded) were fitted to give $k_{rel}=1.070\pm0.010$ (2σ). Error bars assigned the individual data points correspond to 1σ from the spectral analyses.

EGU

EGU
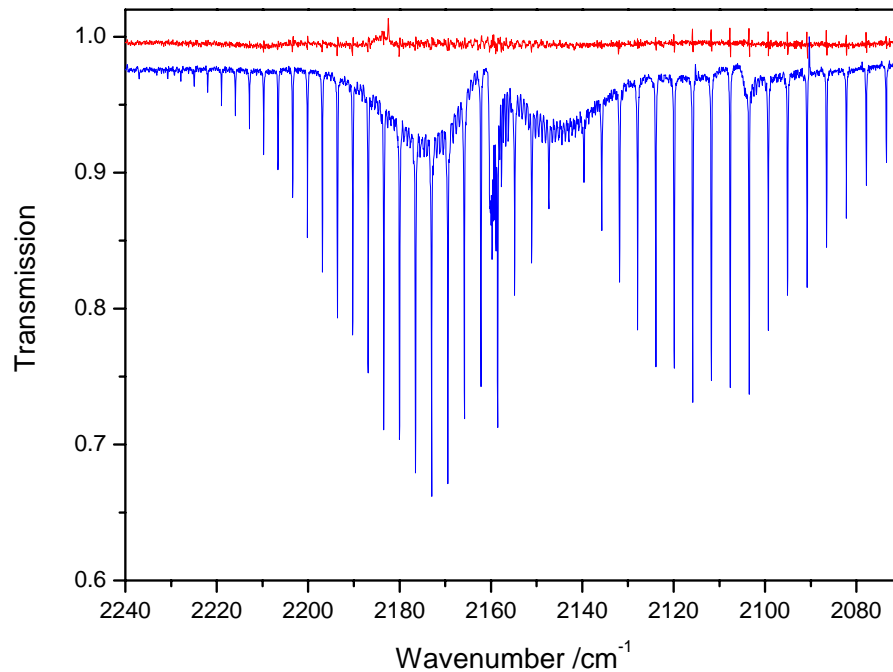
Fig. 4. FT-IR spectrum of the CD stretching region of a $^{12}CH_3Cl$ and CD_3Cl mixture during reaction with Cl atoms. The $v_1(A_1)$ and $2v_5(A_1+E)$ modes of CD_3Cl are overlapped by the sharp vibration-rotation lines of the CO fundamental centred at 2043 cm^{-1}. The topmost curve is the residual of the spectral fitting. Compounds included in the spectral analysis: CD_3Cl, H_2O, HDO, CO and CO_2.

EGU

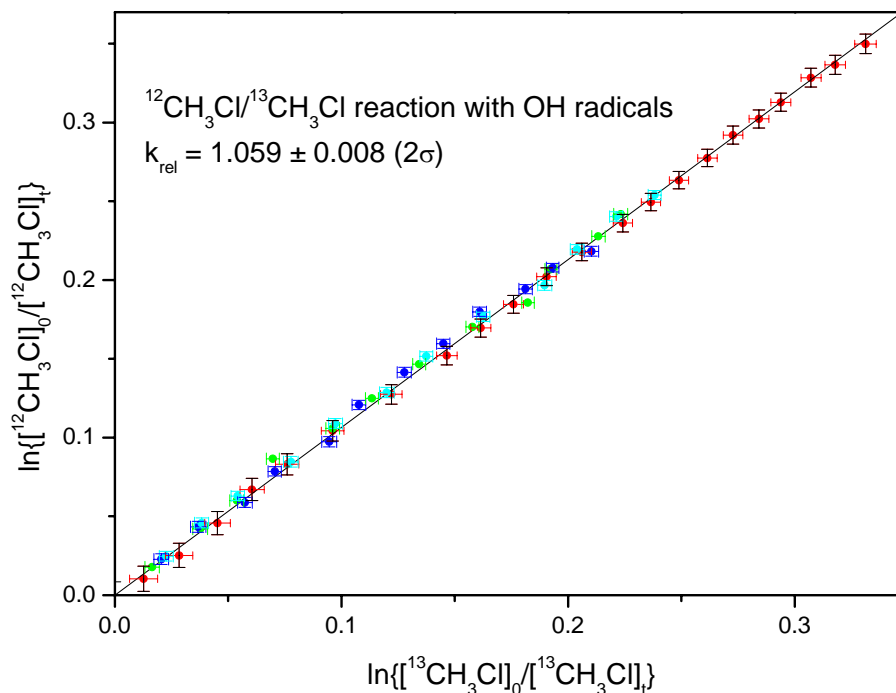**Fig. 5.** Decays of CH_3Cl and CD_3Cl during reaction with Cl atoms at 1013 mbar and 298 K plotted in the form $\ln\{[^{12}CH_3Cl]_0/[^{12}CH_3Cl]_t\}$ vs. $\ln\{[CD_3Cl]_0/[CD_3Cl]_t\}$. 26 data points from 2 experiments (colour coded) were fitted to $k_{rel}=4.91\pm0.07$ (2σ). Error bars assigned the individual data points correspond to 1σ from the spectral analyses.

EGU
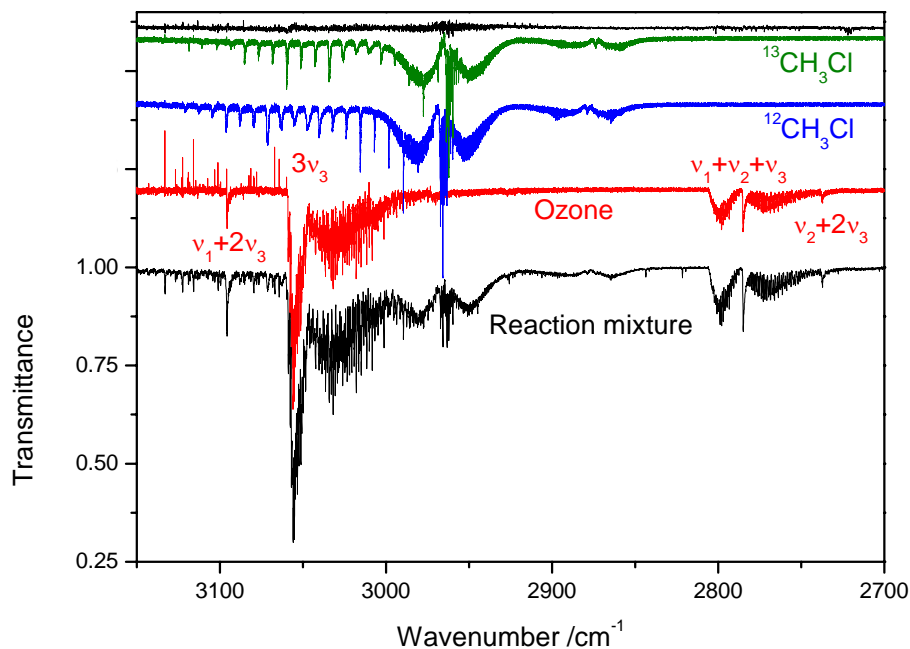
Fig. 6. FT-IR spectrum of the CH stretching region of a CH$_3$Cl and ^{13}CH$_3$Cl mixture during reaction with OH radicals. The reference spectra of O$_3$, ^{12}CH$_3$Cl and ^{13}CH$_3$Cl as well as the residual of the fit have been displaced for clarity. The topmost curve is the residual of the spectral fitting. Compounds included in the spectral analysis: ^{12}CH$_3$Cl, ^{13}CH$_3$Cl, H$_2$O and HCl.

EGU

$^{12}CH_3Cl/^{13}CH_3Cl$ reaction with OH radicals

$k_{rel} = 1.059 \pm 0.008\ (2\sigma)$

x-axis: $\ln\{[^{13}CH_3Cl]_0/[^{13}CH_3Cl]_t\}$

y-axis: $\ln\{[^{12}CH_3Cl]_0/[^{12}CH_3Cl]_t\}$

Fig. 7. Decays of CH_3Cl and CD_3Cl during reaction with OH radicals at 1013 mbar and 298 K plotted in the form $\ln\{[^{12}CH_3Cl]_0/[^{12}CH_3Cl]_t\}$ vs. $\ln\{[CD_3Cl]_0/[CD_3Cl]_t\}$. 58 data points from 4 independent experiments (colour coded) were fitted to $k_{rel}=1.059\pm0.008\ (2\sigma)$. Error bars assigned the individual data points correspond to 1σ from the spectral analyses.
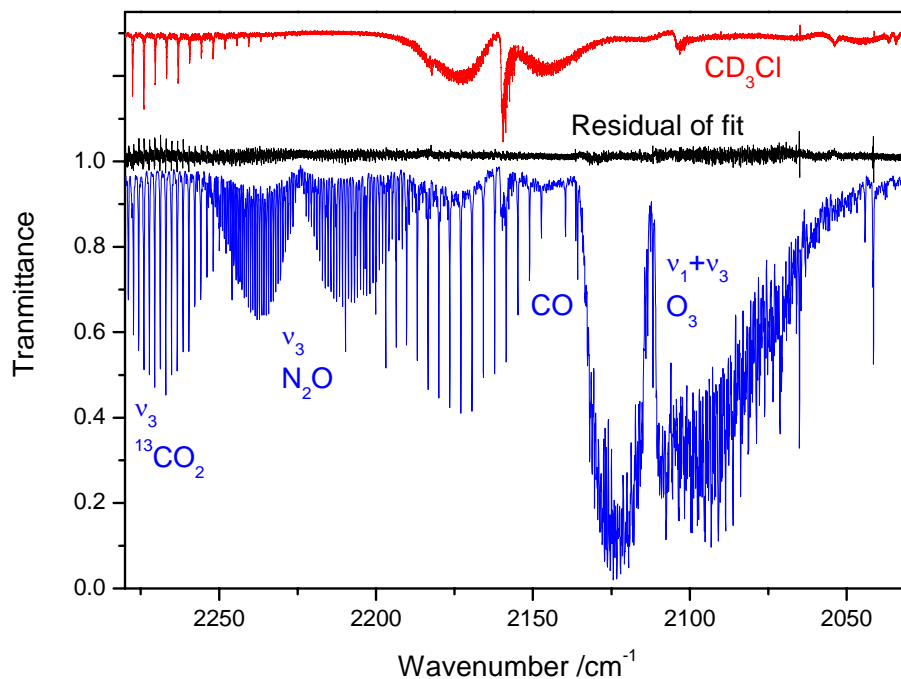
Fig. 8. FT-IR spectrum of the CD stretching region of a CH_3Cl and CD_3Cl mixture during reaction with OH radicals. The spectrum was analyzed in terms of CO_2, CO, N_2O, H_2O and O_3 reference spectra from the HITRAN database and of the shown high resolution reference spectrum of CD_3Cl, which has been shifted for the sake of clarity.
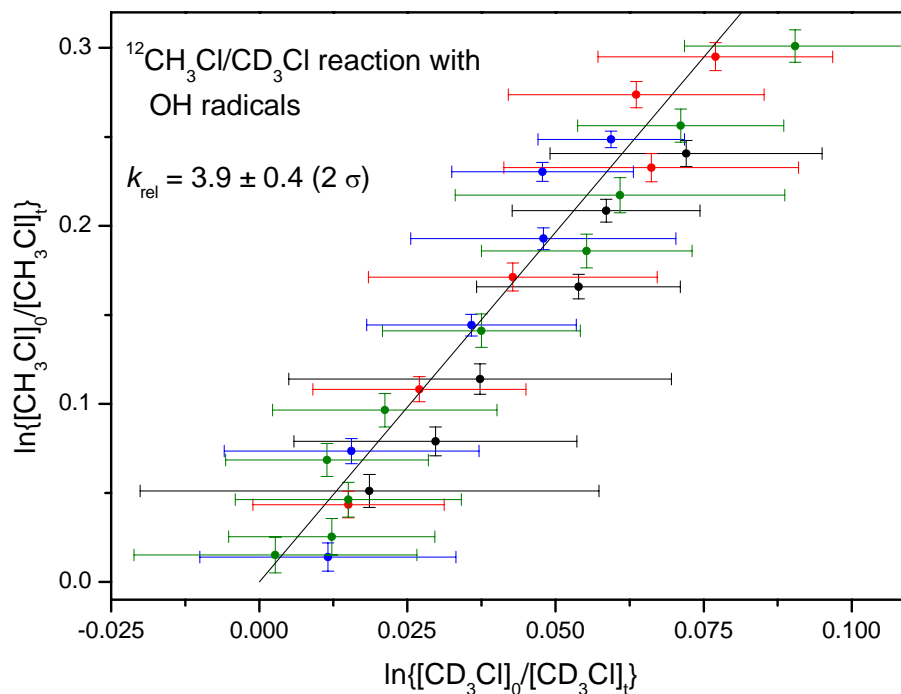
EGU

Fig. 9. Decays of CH_3Cl and CD_3Cl during reaction with OH radicals at 1013 mbar and 298 K plotted in the form $\ln\{[^{12}CH_3Cl]_0/[^{12}CH_3Cl]_t\}$ vs. $\ln\{[CD_3Cl]_0/[CD_3Cl]_t\}$. 28 data points from 4 experiments (colour coded) were fitted to $k_{rel}=3.9\pm0.4$ (2σ). Error bars assigned the individual data points correspond to 1σ from the spectral analyses.